

Time-varying frequency Estimation of narrow-band signals via Extended Kalman Filter and Unscented Kalman Filter

Emanuele Dalla Longa Sergio Gandola

September 2018

Abstract

In this paper the problem of estimating the frequency of a narrow-band harmonic signal embedded in noise is discussed; in particular, Kalman filter-based approaches such as the *Extendend Kalman Filter* (EKF) and the *Unscented Kalman Filter* (UKF). In order to evaluate the achieved estimation quality of the algorithms, two criteria are introduced: the *Performance Index* (PI) and the *Robustness Index* (RI), plus an auxiliary *Convergence Ratio*. Tests have been performed both on recorded real world signals and on generated noisy signals.

1 Introduction

This work explores and compares the capabilities of Kalman filter-based frequency tracking methods such the *Extendend Kalman Filter* (EKF) and the *Unscented Kalman Filter* (UKF) to track the time-varying frequency of a narrow-band harmonic signal. These results are compared with those by Savaresi et al. in [3].

In order to evaluate the achieved estimation quality of the algorithms, two criteria are used: the *Performance Index* (PI) and the *Robustness Index* (RI), described in[3]. An auxiliary *Convergence Ratio* is introduced to better interpret the PI plots.

Two signals are considered: a single frequency sinusoidal signal recorded from the real world and a generated noisy signal with time-varying frequency following a step profile. The algorithm was able to estimate the real world signal with accuracies $\sim 10^{-7}$ and achieve performances consistent with [3].

In the last section the obtained results are shown and discussed, with emphasis on some behaviors which may be due to numerical errors.

2 Previous works

This work builds on [1] for the EKF implementation and on [3] for the performance evaluation. [3] was also used along with [4] for the implementation of the UKF algorithm.

3 Problem statement

Consider the signal :

$$y(t) = s(t) + n(t)$$

where $n(t)$ is a broadband noise (e.g., a white noise) and $s(t)$ a sinusoid of the type

$$s(t) = A \cdot \sin(\Phi(t) + \phi)$$

where $\Phi(t)$ is the instantaneous frequency as described in [2].

The proposed model is constructed from the representation of the signal as a rotating vector in the Cartesian plane with angular velocity $\Phi(t)$. A third-order state space model (ARMA representation) is derived by taking the two projections of the vector along the axes and the instantaneous frequency as state variables:

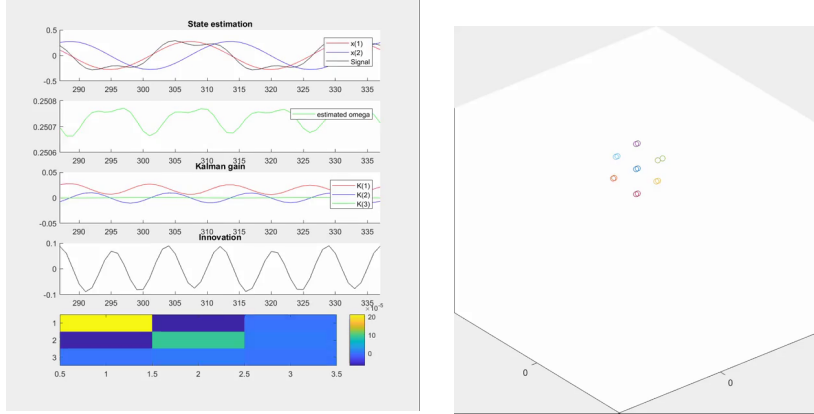
$$\begin{cases} x_1(t+1) = \cos(x_3(t))x_1(t) - \sin(x_3(t))x_2(t) \\ x_2(t+1) = \sin(x_3(t))x_1(t) + \cos(x_3(t))x_2(t) \\ x_3(t+1) = x_3(t) + w(t) \\ y(t) = x_1(t) + v(t) \end{cases}$$

Two uncorrelated, zero mean noises $w(t) \sim WN(0, q)$ and $v(t) \sim WN(0, r)$ have been introduced, where q represent the a-priori variance attributed to the state variables, while r is the a-priori variance attributed to the measurement variable. As proven in [1], the ratio $\sigma = r/q$ alone governs the estimation performances for the EKF, and the reasoning can be extended to the UKF. This parameter regulates the trade-off between convergence quality (high sigma, low state estimation variance) and convergence speed (ability to react quickly to abrupt frequency variations).

We found this to be true experimentally; however, in the last section we show how and when the absolute values of the parameters q and r start to play a relevant role in the algorithm performances with the standard implementation.

4 Proposed approaches

The two approaches used in this paper are the EKF and the UKF. A brief description of the latter is given below.



(a) Signal, estimation, Kalman gain and covariance matrix P^1 . $\omega_{\text{true}} = 0.25076 \text{ rad/sample}$ (1760 Hz)

(b) Evolution of sigma points in the state space

Figure 1: UKF visualizations

4.1 Unscented Kalman Filter

The Unscented Kalman Filter (UKF) is a widely used method to estimate the state vector of a non-linear process, based on the Unscented Transformation, which is a method for calculating the statistics of a random variable which undergoes a nonlinear transformation. It is founded on the intuition that it is easier to approximate a probability distribution than it is to approximate an arbitrary nonlinear function or transformation.

Unscented transformation The sigma points ς are chosen so that their mean and covariance are exactly \hat{x}_{k-1} and P_{k-1} , where \hat{x}_{k-1} is the predicted state vector and P_{k-1} the covariance matrix at the previous instant. Each sigma point is then propagated through the nonlinearity, yielding in the end a cloud of transformed points. The newly estimated mean and covariance are then computed using their statistics, weighted with an optimal set of weights.

Data assimilation step The Kalman gain is computed as

$$K_k = \text{Cov}(\varsigma_k^s, \varsigma_k^m) \cdot \text{Cov}(\varsigma_k^m, \varsigma_k^m)^{-1}$$

where ς_k^s are the sigma points propagated through the state model function and ς_k^m are the sigma points propagated through the measurement model function. A visualization of this is given in Figure 1b.

¹It is interesting to notice how the absolute values of the elements of P are proportional to the slope of the component in the figure: higher rate of change means higher estimation variance.

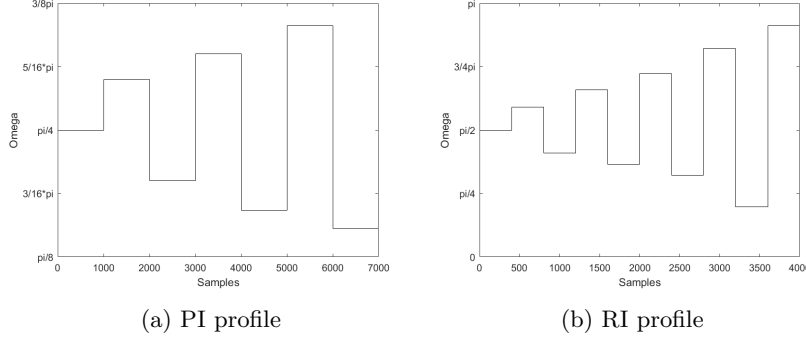


Figure 2: Test signal frequency profile for PI and RI

Then, the new state estimation is computed as:

$$\hat{x}_k = \hat{x}_{k|k-1}^s + K_k \cdot [y_k - \hat{x}_{k|k-1}^m]$$

We add to the estimate of the state vector $\hat{x}_{k|k-1}^s$, weighted mean of ζ_k^s , the innovation, computed as the difference between the measurement y_k and the weighted mean of ζ_k^m , tuned by the Kalman gain K_k .

4.2 Performance evaluation

In order to evaluate the analysis, two different performance indices are introduced: the Performance Index (PI) and the Robustness Index (RI). As shown in the following sections, the two indices give us a metric that can be extended to every frequency tracker: they are indeed related to the capability of the tracker to attain low error at steady state, and the capability to converge, possibly rapidly, after a sudden change of the signal frequency.

4.2.1 Performance Index

The goal of the Performance Index is to characterize the trade-off between the algorithm convergence rate and the error at steady-state. We can define two different intervals :

Transient Interval (T_t) related to the error during transient conditions

Steady State Interval (T_{ss}) related to the error at steady state

The length of $T_t(i)$ and $T_{ss}(i)$ are different for each i^{th} step, in order to take into account the speed of convergence (the higher the step, the slower the convergence). The duration of these time steps are taken from [3, Table 1]. Given $\hat{\omega}(t)$, the estimated instantaneous frequency at time t , it is possible to compute the *MSE* of the estimated signal with the formula below:

$$MSE(e(t)) = MSE(\omega(t) - \hat{\omega}(t)) = \sum_{t=1}^N (\omega(t) - \hat{\omega}(t))^2 \quad (1)$$

Where N is the number of samples. For each i^{th} step we can define two separate errors, the transient error $e_{t,i}$ and the steady state error $e_{ss,i}$. Each error is computed within the corresponding portion of time interval of the step. We then compute $MSE(e_{t,i})$ and $MSE(e_{ss,i})$ as defined in (1). Then, the PI is computed as the tuple

$$\left\{ \frac{1}{N_{\text{step}}} \sum_{i=0}^{N_{\text{step}}} MSE(e_{t,i}), \frac{1}{N_{\text{step}}} \sum_{i=0}^{N_{\text{step}}} MSE(e_{ss,i}) \right\}$$

4.2.2 Robustness Index

The purpose of the Robustness Index is to evaluate the capability of the estimation method to converge after large variations of the signal frequency. Given a frequency profile (which for this article will be the one described in Figure 2b), the RI is defined as a vector of length n , where n is the number of steps in the profile. Each element RI_i of the vector is the number of times the algorithm converged until step i , then diverged. The convergence is determined by heuristic thresholding of the MSE.

4.2.3 Convergence ratio

This is a novel performance metric introduced in this paper, to preserve the information about the non-converged iterations which are filtered in the plot of the PI. It is an approximation of the pointwise ratio $\frac{\text{Converged Iterations}}{\text{All Iterations}}$ of the algorithm as a function of σ . First, a boolean vector

$$c^b | c_i^b = 1 \iff \text{the algorithm converged with } \sigma_i$$

is introduced. Let c^{cum} be the cumulative sum of c^b and g a gaussian kernel. We have

$$c^{\text{cum}} * \nabla g \approx \frac{dc^{\text{cum}}}{d\sigma}$$

where $\frac{dc^{\text{cum}}}{d\sigma}$ is proportional to the convergence ratio.

5 Experiment setup

5.1 Signal generation

5.1.1 Real signal

The algorithm has been tested on signals recorded from the real world. A single frequency sinusoidal signal has been generated with a smartphone, and recorded

	q	σ	MSE
EKF	1×10^{-11}	1×10^8	3.60×10^{-7}
UKF	1×10^{-11}	1×10^8	4.53×10^{-7}
	(a) 440 Hz		
	q	σ	MSE
EKF	1×10^{-11}	1×10^9	4.29×10^{-7}
UKF	1×10^{-11}	1×10^9	4.41×10^{-7}
	(b) 880 Hz		
	q	σ	MSE
EKF	1×10^{-11}	1×10^9	8.69×10^{-8}
UKF	1×10^{-11}	1×10^9	9.52×10^{-8}
	(c) 1760 Hz		

Table 1: Frequency estimation performances on a real world sinusoidal signal

through a low quality, built-in laptop microphone in a medium sized bedroom. Three sinusoids have been generated: 440 Hz, 880 Hz, 1760 Hz. The best results that could be obtained are shown in Table 1.

5.1.2 Generated noisy signal

For the PI and RI tests, the signal has been generated with the following formula:

$$\begin{aligned}
y &= \sin(\Phi(t) + x_5(t)) + \sigma_{\text{noise}} (\sin^2(x_1 t) + \sin^3(x_2 t) + \sin^4(x_3 t) + x_4) \\
x_1, x_2, x_3 &\sim \mathcal{U}(0, \pi) \\
x_4 &\sim \mathcal{N}(0, 1) \\
x_5(t) &\sim \mathcal{N}(0, \sigma_{\omega, \text{noise}} \cdot \omega_0)
\end{aligned}$$

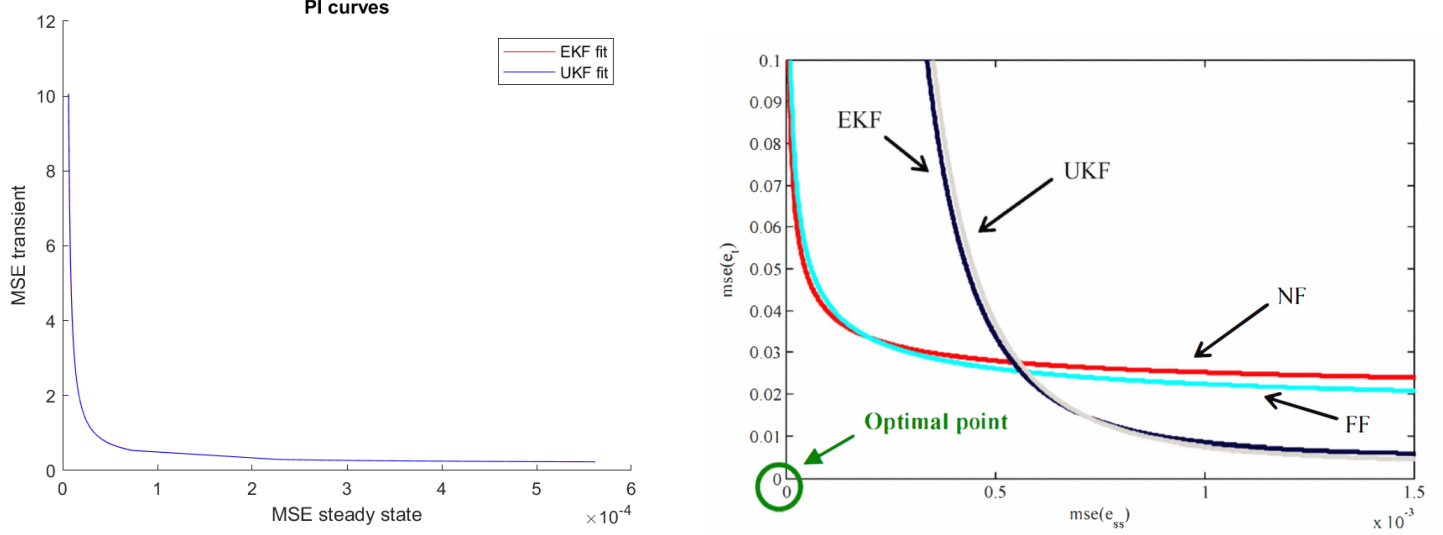
and σ_{noise} is a parameter which regulates the SNR and $\sigma_{\omega, \text{noise}}$ a parameter which regulates the phase noise as a percentage of the initial frequency.

The experiments have been performed on a signal with a step varying frequency. For the PI, the following profile has been used (Figure 2a):

$$\begin{aligned}
\omega_0 &= \frac{\pi}{4}, \quad \omega_i = \omega_{i-1} + s_i \\
s_i &= \left\{ \frac{\pi}{20}, \frac{-\pi}{10}, \frac{\pi}{8}, \frac{-\pi}{6.5}, \frac{\pi}{5.5}, \frac{-\pi}{5} \right\}
\end{aligned}$$

While this is the profile used for the RI (Figure 2b):

$$\begin{aligned}
\omega_0 &= \frac{\pi}{2}, \quad \omega_i = \omega_{i-1} + s_i \\
s_i &= \left\{ \frac{\pi}{11}, \frac{-\pi}{5.5}, \frac{\pi}{4}, \frac{-\pi}{3.4}, \frac{\pi}{2.8}, \frac{-\pi}{2.5}, \frac{\pi}{2}, \frac{-\pi}{1.6}, \frac{\pi}{1.4} \right\}
\end{aligned}$$



(a) Our results. These have been obtained by a Least Square fit of a generic hyperbola $a + \frac{b}{x+c}$ over the raw data shown in Table 2, $q = 1 \times 10^{-6}$, SNR 46 dB. $MSE_{fit} = 6.3 \times 10^{-3}$

(b) Results from [3, Figure 3]

Figure 3: PI curves comparison

5.2 Tests

5.2.1 PI

Tests for the PI have been performed with different σ_{error} s, corresponding to these SNRs:

$$\{\infty, 46\text{dB}, 22\text{dB}, 15\text{dB}\}$$

and $\sigma_{\omega, \text{noise}} = 0$. The σ parameter has been evaluated from 1×10^3 and 1×10^{-4} with a logarithmically spaced profile. For each σ a point in the e_{ss} , e_t plane has been drawn in Figure 2. Outliers have been removed by heuristic thresholding.

5.2.2 RI

For RI, tests have been performed in low noise conditions (Figure 7a) and in high noise conditions (Figure 7b). This test is visualized in Figure 6.

6 Results

In this section the results obtained from the experiments are discussed.

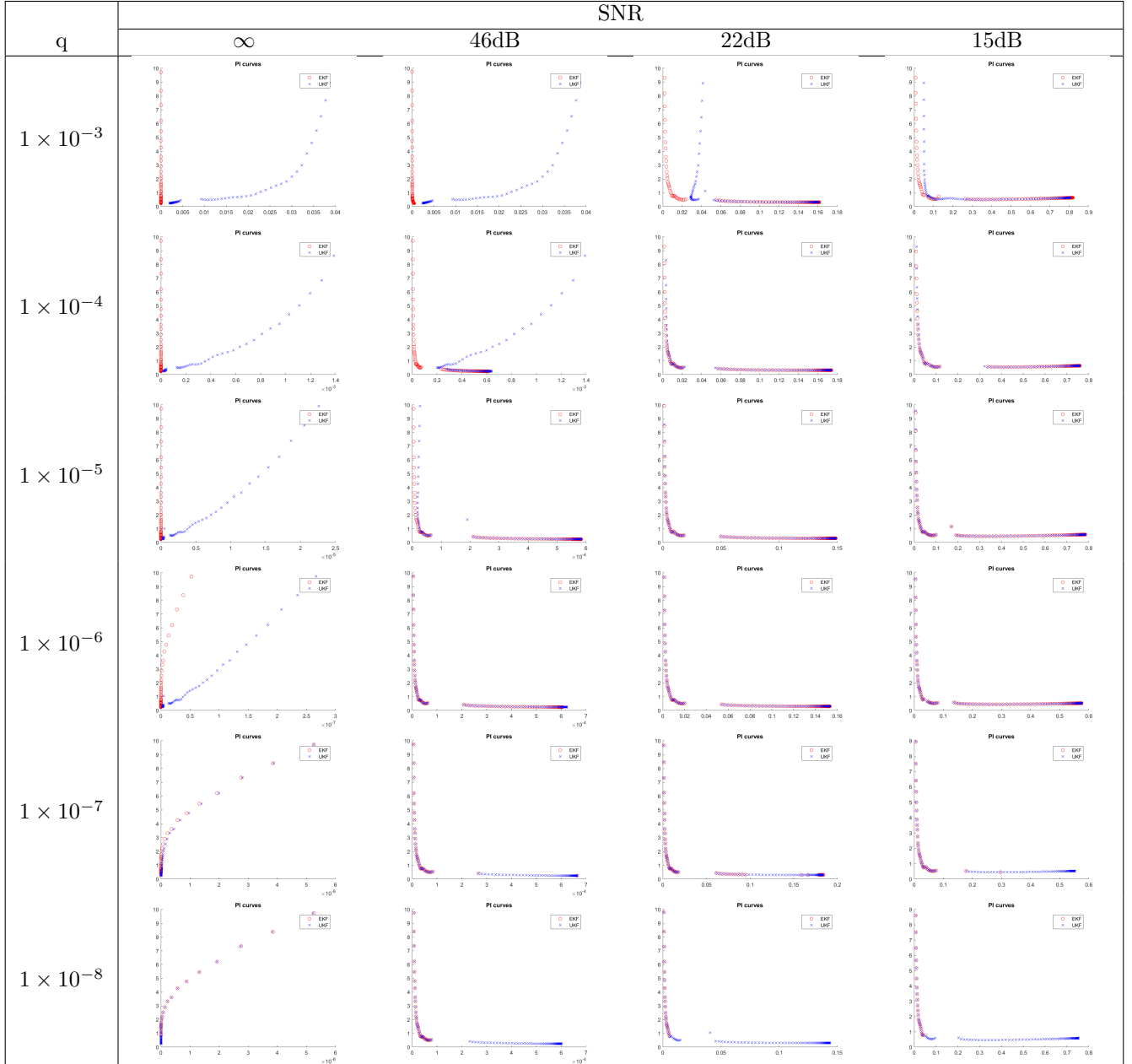


Table 2: Obtained curves for the PI. On the x axis is the e_{ss} , while on the y axis is the e_t . Thresholding has been applied to remove non converged iterations.

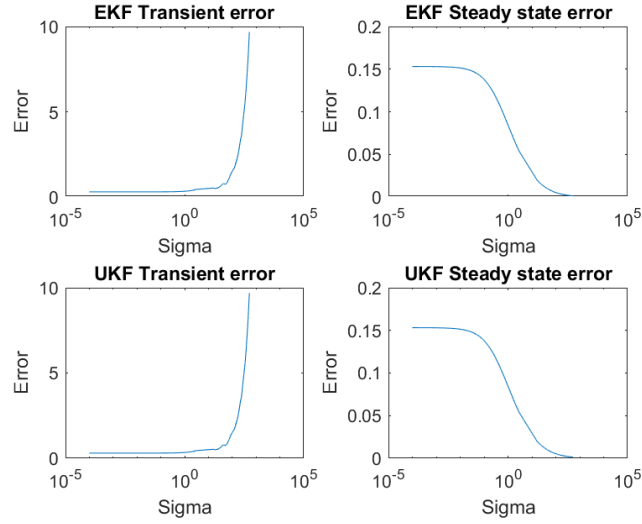


Figure 4: The error as a function of σ (SNR 22 dB). It is evident that σ regulates the tradeoff between convergence speed and quality.

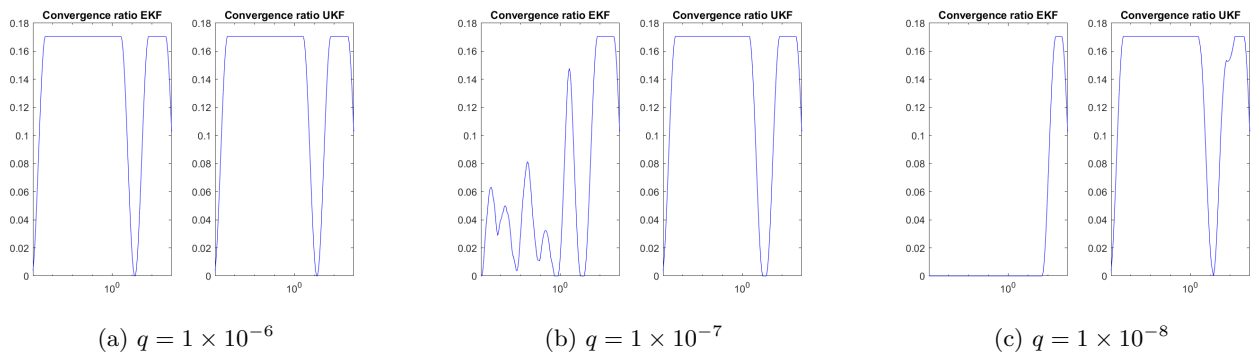


Figure 5: Convergence ratios as a function of σ (22 dB)

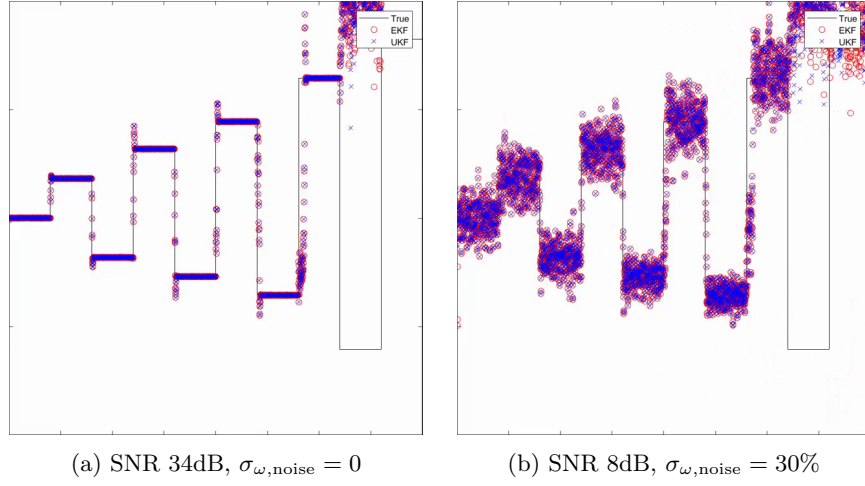


Figure 6: Visualization of some predictions for the computation of the RI index with $\sigma = 1 \times 10^1$, $q = 1 \times 10^{-5}$

6.1 PI

In Figure 3 the smoothest fit for the PI curve is shown. It is really similar to [3, Figure 3]. The original noise profile and the original parameters are unknown; our best e_t is one orders of magnitude bigger than the best one by Savaresi et al. (2.5×10^{-1}), but we are able to obtain a steady state error of 3.28×10^{-6} , two orders of magnitude smaller. With no noise, the best performances for both EKF and UKF are of the order of $e_{ss} \sim 10^{-26}$.

In Table 2 we see the effects of q . These may be due to finite arithmetic precision. In the lower-right portion of the image, the shape of the curve is more or less invariant, even in high noise conditions; however, the EKF stops converging at really small qs and small σs (absence of red points). This is highlighted also in Figure 5. We can observe that in the Riccati equation, the matrix $HPH^T + q$ is inverted. With low noise and low q , both terms are really small ($\sim 10^{-8}$ before diverging), pointing to a possible numerical error.

We can also see how, for big qs and big σs , the UKF changes behavior abruptly as r grows, (e.g., in Figure 2, $q = 1 \times 10^{-3}$, 22 dB, or $q = 1 \times 10^{-4}$ 46 dB), without compromising on convergence ratios, and maintaining comparable performances with the EKF. Since r is summed to the propagated sigma points, having an r 3-7 orders of magnitude bigger than the terms of $\text{Cov}(\zeta_k^s, \zeta_k^m)$ and $\text{Cov}(\zeta_k^m, \zeta_k^m)$ may be the source of the weird behavior, given the variable resolution of the floating point representation.

There is also a valley in the convergence ratio with $15 \leq \sigma \leq 30$ for both algorithms, which we were not able to explain.

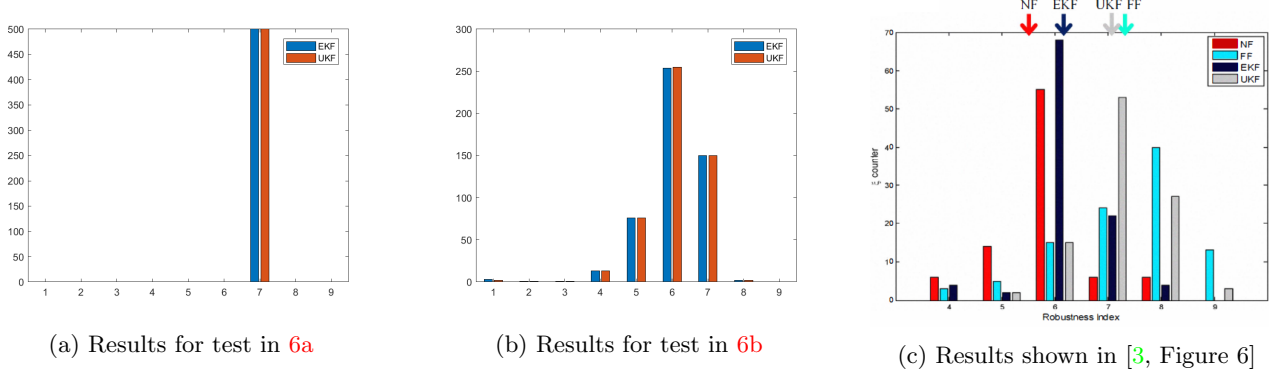


Figure 7: Results for simulations shown in Figure 6, 500 iterations

6.2 RI

Multiple simulations have been performed with several parameter combinations. In Figure 6 two visualizations of the prediction are shown for the two algorithms with two different SNRs. In Figure 7 are the results obtained. With low noise the algorithm always converged until step 7, then getting stuck at π (Figure 7a). With high noise, although the performance are worsened, we see that the algorithm is sometimes able to converge at step 8.

References

- [1] S. Bittanti and S. Savaresi. “On the Parameterization and Design of an Extended Kalman Filter Frequency Tracker”. In: *IEEE transactions on automatic control* 45.9 (2000), pp. 1718–1724.
- [2] B. Boashash. “Estimating and Interpreting the instantaneous frequency of a signal”. In: *Proceedings of the IEEE* 80.4 (1992), pp. 540–568.
- [3] S. Savaresi et al. “Frequency estimation of narrow band signals in Gaussian noise via Unscented Kalman Filter”. In: *49th IEEE Conference on Decision and Control* (2010), pp. 2869–2874.
- [4] Gabriel A. Terejanu. *Unscented Kalman Filter Tutorial*. URL: <https://www.cse.sc.edu/~terejanu/files/tutorialUKF.pdf>.